

Lead-strontium titanate glass ceramics: I – crystallization and microstructure

ASHOK K. SAHU*, DEVENDRA KUMAR†, OM PARKASH

Department of Ceramic Engineering, Institute of Technology, Banaras Hindu University, Varanasi, 221005, India

E-mail: ashok@magnum.barc.ernet.in

E-mail: dev_ceramic@yahoo.co.in

Published online: 10 March 2006

The crystallization behaviour of glasses in the system $[(\text{Pb}_{1-x}\text{Sr}_x)\text{O}\cdot\text{TiO}_2]\text{-}[2\text{SiO}_2\cdot\text{B}_2\text{O}_3]\text{-}[\text{K}_2\text{O}]\text{-}[\text{BaO}]$ ($0.2 \leq x \leq 0.9$) have been studied. Perovskite titanate was found to be the major phase in all the glass ceramic samples investigated. The actual composition of crystalline phases could not be confirmed on the basis of shift in the X-ray diffraction (XRD) peak positions because of similar effects due to solid solution formation and strain due to crystal clamping. Comparison of the observed intensities of various XRD peaks of the perovskite titanate phase with the calculated intensities for $(\text{Pb}_{1-x}\text{Sr}_x)\text{TiO}_3$ with same lead/strontium ratio confirmed the formation of lead strontium titanate solid solution. Microstructural characteristics of various glass ceramics are also discussed. The advantages of using K_2O and BaO as additives instead of only K_2O are also discussed. © 2006 Springer Science + Business Media, Inc.

1. Introduction

The development of glass ceramics containing perovskite titanate solid solutions crystals in lieu of pure and undoped phase is expected to result in superior properties as it combines the advantages of solid solution formation and glass ceramic processing [1]. Glass ceramics containing undoped perovskite titanate phases such as PbTiO_3 [2–9] and SrTiO_3 [10–19] have been extensively investigated. A few attempts have been made to develop perovskite titanate solid solution crystals in glass matrix [4, 5, 8, 20–22] but without any success. Recently we reported the crystallization of $(\text{Pb}, \text{Sr})\text{TiO}_3$ solid solution phase in borosilicate glass matrix [23, 24]. We have observed that $(\text{Pb}, \text{Sr})\text{TiO}_3$ phase can be crystallized in the system $[(\text{Pb}_{1-x}\text{Sr}_x)\text{O}\cdot\text{TiO}_2]\text{-}[2\text{SiO}_2\cdot\text{B}_2\text{O}_3]\text{-}[\text{K}_2\text{O}]$ with suitable choice of composition and heat treatment schedule. On the basis of the calculated and observed intensities of various X-ray diffraction (XRD) peaks, the composition of the crystallites was confirmed to be $(\text{Pb}, \text{Sr})\text{TiO}_3$ solid solution which was further supported by Curie temperature of the crystalline phases developed. However, preparation of transparent bulk glasses thicker than a few millimeters was very difficult. Very high cooling rate is required to prepare thick transparent glasses. In all the glasses prepared, K_2O was present which acts as network

modifier and expected to introduce a large number of non-bridging oxygen ions in the glass structure. This reduces the viscosity of the melt, making it difficult to get thick transparent glasses under ordinary conditions by conventional melt-quench method. We have also observed that in borosilicate glass system, addition of equivalent amounts of K_2O and BaO results in easy glass formation and better crystallization of perovskite phase [19]. Therefore, in a search for better glass ceramic systems it was considered worthwhile to prepare and study the crystallization behaviour of glasses in the system $[(\text{Pb}_{1-x}\text{Sr}_x)\text{O}\cdot\text{TiO}_2]\text{-}[2\text{SiO}_2\cdot\text{B}_2\text{O}_3]\text{-}[\text{K}_2\text{O}]\text{-}[\text{BaO}]$ and the microstructural characteristics of resulting glass ceramics. This paper presents the results of our investigation. The glass and glass ceramics developed in the present investigation are expected to show superior properties than the glass and glass ceramics prepared earlier [23, 24].

2. Experimental procedure

Glasses in the system $[(\text{Pb}_{1-x}\text{Sr}_x)\text{O}\cdot\text{TiO}_2]\text{-}[2\text{SiO}_2\cdot\text{B}_2\text{O}_3]\text{-}[\text{K}_2\text{O}]\text{-}[\text{BaO}]$ were prepared with $x = 0.2$ to 1.0 with a stepwise increment of 0.1. Well mixed and dried powders containing appropriate amounts of reagent grade PbO , SrCO_3 , TiO_2 , H_3BO_3 , K_2CO_3 and BaCO_3 were

*Present Address: Materials Processing Division, Bhabha Atomic Research Centre, Mumbai, 400085, India.

†Author to whom all correspondence should be addressed.

0022-2461 © 2006 Springer Science + Business Media, Inc.

DOI: 10.1007/s10853-006-3642-3

melted in pure alumina crucibles. The melting temperature of all the glasses was found to be in the temperature range 1100–1300°C. The melts were kept for 1 h at the respective melting temperatures for homogenization. The melts were quenched by pouring into an aluminium mould and pressing with a thick aluminium plate. The glasses were then annealed at 400°C for 3 h. Differential thermal analysis (DTA) was done using a NETZSCH Simultaneous Thermal Analyzer 409 from room temperature (~27°C) to 900°C employing a heating rate of 10°C/min to determine glass transition and crystallization temperatures.

On the basis of differential thermal analysis (DTA) results, glasses were crystallized by subjecting them to various heat treatment schedules. X-ray diffraction patterns for resulting glass ceramic samples were recorded employing a Rich-Seifert ID 3000 diffractometer using Cu K α radiation. The crystalline phase(s) in each glass ceramic sample was (were) identified by comparing its XRD pattern with standard patterns of various crystalline phases which might have formed from different constituent oxides of the glass. In a typical powder X-ray diffraction pattern, the position of XRD peaks (2θ), i.e., diffraction directions are determined solely by the shape and size of unit cell. The intensities of diffracted beams are determined by the positions of the atoms within the unit cell. In perovskite solid solution ceramics such as (Pb $_{1-x}$ Sr $_x$)TiO $_3$, if there is large difference between the atomic scattering factors of substituent and substituted atoms in the unit cell, then the intensities of different XRD lines change with change in concentration of substituent ions along with crystal structure and lattice parameter(s). The atomic scattering factors of lead and strontium ions are quite different. Therefore, the relative intensity of XRD peaks should change with x in (Pb $_{1-x}$ Sr $_x$)TiO $_3$ solid solution. Hence an effort was made to calculate the intensity of different XRD peaks for various compositions in the (Pb $_{1-x}$ Sr $_x$)TiO $_3$ solid solution series as reported earlier [23]. A few glass ceramic samples were selected to study the variation of intensity of various XRD lines of their crystalline perovskite phase with varying Pb $^{2+}$ /Sr $^{2+}$ ratio (or x) in the initial glass composition. The observed intensity of XRD peaks of the crystalline phase precipitated in different glass ceramics was compared with calculated intensity of the corresponding XRD peaks. The glass ceramic samples were polished, etched with a solution containing equal volumes of 30% HNO $_3$ and 20% HF for 60 seconds and then coated with a thin film of gold for scanning electron microscopy (SEM) observations (Model JEOL 840A).

3. Results and discussion

3.1. Differential thermal analysis (DTA) studies

DTA traces of a few selected glasses are presented in Fig. 1. For all the glasses there is a shift in the base line in the temperature range 540–690°C, depending

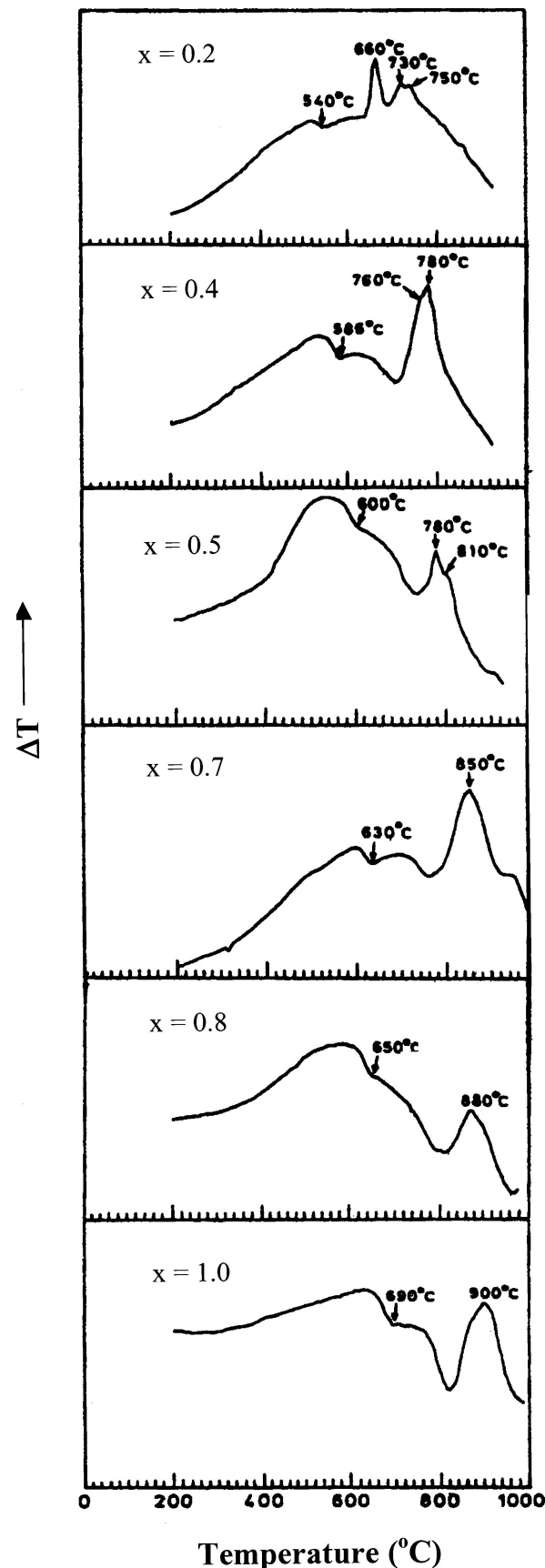


Figure 1 DTA patterns of glasses in the system 65[(Pb $_{1-x}$ Sr $_x$)O·TiO $_2$] - 25[2SiO $_2$ ·B $_2$ O $_3$] - 5[K $_2$ O] - 5[BaO].

TABLE I Observed DTA peaks of different glass samples in the system $[(\text{Pb}_{1-x}\text{Sr}_x)\text{O}\cdot\text{TiO}_2] - [\text{2SiO}_2\cdot\text{B}_2\text{O}_3] - [\text{K}_2\text{O}] - [\text{BaO}]$

Composition (x)	Glass code	DTA Peaks ($^{\circ}\text{C}$)			
		T_g	T_{C1}	T_{C2}	T_{C3}
0.2	8P5K	540	660	730	750
0.3	7P5K	560	–	740	770
0.4	6P5K	585	–	760	780
0.5	5P5K	600	–	780	810
0.6	4P5K	610	–	–	850
0.7	3P5K	630	–	–	850
0.8	2P5K	650	–	–	880
0.9	1P5K	660	–	–	850
1.0	5T5K	690	–	–	900

on the composition. The shift in base line representing change in specific heat is attributed to the glass transition. The glass transition temperature, T_g of different glasses are listed in Table I. The glass transition temperature is found to increase with increasing concentration of SrO. This may be due to increase of viscosity of the melt with increasing SrO concentration in the glass. For glass sample with $x = 0.2$ three exothermic crystallization peaks T_{C1} , T_{C2} and T_{C3} appear in DTA plot whereas for other lead rich glass compositions ($x \leq 0.5$) two exothermic peaks (T_{C2} and T_{C3}), fused together appear in the DTA plots. For SrO rich compositions ($x > 0.5$), the two peaks (T_{C2} and T_{C3}) merge together and give a single exothermic peak which shifts to higher temperature with increasing SrO concentration. Later XRD studies of the glass ceramic samples revealed that T_{C1} is due to crystallization of PbTi_3O_7 phase where as T_{C2} and T_{C3} are due to the crystallization of the precursor perovskite phase and transformation of the precursor perovskite phase to stable solid solution lead strontium titanate perovskite phase respectively. From the DTA studies of glasses with only K_2O as additive [23] and the same system with K_2O and BaO as additive, in the present work, it was observed that the glass transition temperature (T_g) of glasses with same $\text{Pb}^{2+}/\text{Sr}^{2+}$ ratio are nearly equal irrespective of whether it has only K_2O or K_2O and BaO as additives. However, their crystallization temperatures (T_C 's) are quite different. Crystallization temperatures are higher for glasses with K_2O and BaO as additives than that of the glasses with only K_2O . Nucleation temperature (T_N) of a glass is generally considered 50°C above the glass transition temperature by glass technologists. The nucleation and crystallization temperatures are closer for the glasses of K_2O system. Since the crystallization temperature is very close to T_N , high cooling rate is required to avoid crystallization during quenching of the melt for formation of glasses and making of bulk glass sample is difficult. Since T_N and T_C are closer to each other, one can't have control over size of crystallites as nucleation and growth would be occurring simultaneously during heat treatment of these glasses. In case of K_2O and BaO system where T_N and crystallization temperature are widely separated, not only transparent glasses can be formed with relatively lower

cooling rate of the melt but better control over crystallite size can also be exercised.

3.2. X-ray diffraction (XRD) and crystallization studies

On the basis of DTA results, glass samples were subjected to various heat treatment schedules in the temperature range 650 to 900°C . As the glass transition temperature and crystallization temperature (T_{C3}) were found to increase with increasing concentration of SrO in the initial glass, the lead rich glasses were heat treated at a few selected temperatures in the temperature range 650 – 800°C whereas strontium rich glasses were heat treated in the temperature range 750 – 900°C . The phase development in these glass ceramics with crystallization temperature determined from XRD data is summarized in Table II. All the glass ceramics studied under present investigation can be broadly classified into two categories; lead rich compositions, i.e., with $x \leq 0.5$ and strontium rich compositions, i.e., with $x > 0.5$. Perovskite titanate was found to be the major phase in all the glass ceramic samples but the crystal structure of perovskite titanate phase was tetragonal similar to lead titanate for lead rich compositions and was found to be cubic similar to strontium titanate for strontium rich compositions. Powder X-ray diffraction patterns of some representative glass ceramic samples prepared from a lead rich glass ($x = 0.2$) are presented in Figs 2 and 3. Glass with $x = 0.2$, i.e., 8P5 K was heat treated at 650 , 700 and 750°C for 3 h each and thus three glass ceramic samples were prepared. All three glass ceramic samples were found to have perovskite titanate as the major phase (Fig. 2). A shift in XRD peak positions from that of undoped PbTiO_3 which is reflected in the values of their lattice parameters (Table III) was observed. This shift may be due to the formation of $(\text{Pb}, \text{Sr})\text{TiO}_3$ solid solution crystallites and/or strain due to crystal clamping. The only change in these glass ceramics is in the minor phase. The glass ceramics obtained at 650 and 700°C were found to have PbTi_3O_7 as minor phase. Trace amount of PbB_2O_4 was also observed in the glass ceramics obtained at 650°C . The glass ceramic sample obtained at 750°C was found to have traces of rutile (TiO_2) and strontium borate ($\text{Sr}_2\text{B}_2\text{O}_5$). If one takes into account both DTA plot (Fig. 1) and XRD patterns of glass ceramic samples in the temperature range 650 to 750°C , it can be said that initiation of crystallization of both PbTi_3O_7 and perovskite titanate phase has taken place simultaneously. However, the completion of crystallization of PbTi_3O_7 phase takes place either in a short duration of time or upto a slightly higher temperature and perovskite titanate phase continues to crystallize with time. This results in crystallization of desired perovskite titanate as the major phase and PbTi_3O_7 as the minor phase in the resulting glass ceramic sample. When the perovskite titanate phase starts growing the availability of titanium ions for the crystallization of PbTi_3O_7 reduces which in turn stops its crystallization. To study the effect

TABLE II Heat treatment schedules and crystalline phases of different glass ceramic samples in the system $[(\text{Pb}_{1-x}\text{Sr}_x)\text{O}\cdot\text{TiO}_2] - [2\text{SiO}_2\cdot\text{B}_2\text{O}_3] - [\text{K}_2\text{O}] - [\text{BaO}]$

Glass code	Heat treatment schedules			Crystalline phase(s)	Glass ceramic code
	Heating rate ($^{\circ}\text{C}/\text{min}$)	Holding temperature ($^{\circ}\text{C}$)	Holding time (h)		
8P5K	5	650	3	P+PT ₃ *+PB*	8P5K650
	5	700	3	P + PT ₃ *	8P5K700
	5	750	3	P+ R* +SB*	8P5K750
	5	750	6	P	8P5K750S
	5	750	12	P + PT ₃ *	8P5K750T
7P5K	5	700	3	P + PT ₃ *	7P5K700
	5	750	3	P	7P5K750
	5	800	3	P + PT ₃ * +R*	7P5K800
6P5K	5	700	3	P + PT ₃ *	6P5K700
	5	750	3	P + PT ₃ * +R*	6P5K750
	5	750	6	P	6P5K750S
	5	750	12	P	6P5K750T
	5	800	3	P + R*	6P5K800
5P5K	5	700	3	P + PT ₃ *	5P5K700
	5	750	3	P+PT ₃ * +PB*	5P5K750
	5	800	3	P + R*	5P5K800
4P5K	5	750	3	P+PT ₃ *+PB*	4P5K750
	5	800	3	P + R*	4P5K800
	5	850	3	P	4P5K850
3P5K	5	800	3	P	3P5K800
	5	850	3	P + U*	3P5K850
2P5K	5	800	3	P + U*	2P5K800
	5	850	3	P + U*	2P5K850
1P5K	5	800	3	P + PT ₃ *	1P5K800
	5	850	3	P + U*	1P5K850
ST5K	5	850	3	ST + U*	ST5K850
	5	900	3	ST + R +U*	ST5K900

P = Perovskite titanate; PT₃ = PbTi₃O₇; R = TiO₂ (Rutile); SB = Sr₂B₂O₅; PB = PbB₂O₄; ST = SrTiO₃; U = Unidentified phase; *Trace amount.

of holding time on phase and microstructure development, the glass was heat treated at 750 $^{\circ}\text{C}$ for 6 and 12 h. 6 and 12 h heat treatments resulted in development of perovskite titanate as the major phase with trace amount of PbTi₃O₇ (Fig. 3). The lattice parameters ‘*c*’, ‘*a*’ and *c/a* of the perovskite titanate phase developed in glass ceramic samples of the glass 8P5K do not change much with crystallization temperature as the temperature is increased from 650 to 750 $^{\circ}\text{C}$ (Table III). The lattice parameters were also not affected by extended holding time, i.e., 6 and 12 h. This indicates that a stable perovskite phase is developed with 3 h of holding time, which does not undergo any transformation. The only change observed is in terms of minor phase. The observed lattice parameters, both ‘*c*’ and ‘*a*’ were found to be slightly greater than that reported for corresponding ceramics. The axial ratio, *c/a* was also found to be in good agreement with the reported values of corresponding ceramics [26].

The glass ceramic samples 7P5K700, 7P5K750 and 7P5K800 were prepared by heat treatment of the glass 7P5K at 700, 750 and 800 $^{\circ}\text{C}$ for 3 h respectively. The glass ceramic 7P5K700 was found to have perovskite titanate as the major phase with a trace amount of PbTi₃O₇ along with a few low intensity lines of unidentified phase. Perovskite titanate is the only phase observed in case of glass ceramic sample 7P5K750. However, for the glass ceramic sample 7P5K800, trace amounts of PbTi₃O₇ and

TABLE III Crystal structure, lattice parameters and axial ratio of perovskite titanate phase in different glass ceramic samples of the glass $[(\text{Pb}_{0.8}\text{Sr}_{0.2})\text{O}\cdot\text{TiO}_2] - [2\text{SiO}_2\cdot\text{B}_2\text{O}_3] - [\text{K}_2\text{O}] - [\text{BaO}]$ crystallized at different temperatures. Reported values for (Pb_{0.8}Sr_{0.2})TiO₃ ceramic are *c* = 3.983 Å, *a* = 3.864 Å and *c/a* = 1.030 (Ref. [26])

Glass ceramic	Crystal structure	Lattice parameters		Axial ratio (<i>c/a</i>)
		<i>c</i> (Å)	<i>a</i> (Å)	
8P5K650	Tetragonal	4.018 ± 0.001	3.905 ± 0.001	1.029
8P5K700	Tetragonal	4.022 ± 0.002	3.916 ± 0.002	1.027
8P5K750	Tetragonal	4.021 ± 0.002	3.912 ± 0.002	1.027
8P5K750S	Tetragonal	4.033 ± 0.003	3.918 ± 0.003	1.029
8P5K750T	Tetragonal	4.021 ± 0.002	3.916 ± 0.002	1.027

rutile are also observed besides perovskite titanate as the major phase. Perovskite titanate is the major phase in all the above glass ceramic samples. The crystalline phase developed was found to have tetragonal crystal structure. No significant variation in the values of lattice parameters was observed with crystallization temperature. The values of lattice parameters were found to be in good agreement with the reported values of corresponding ceramics [26].

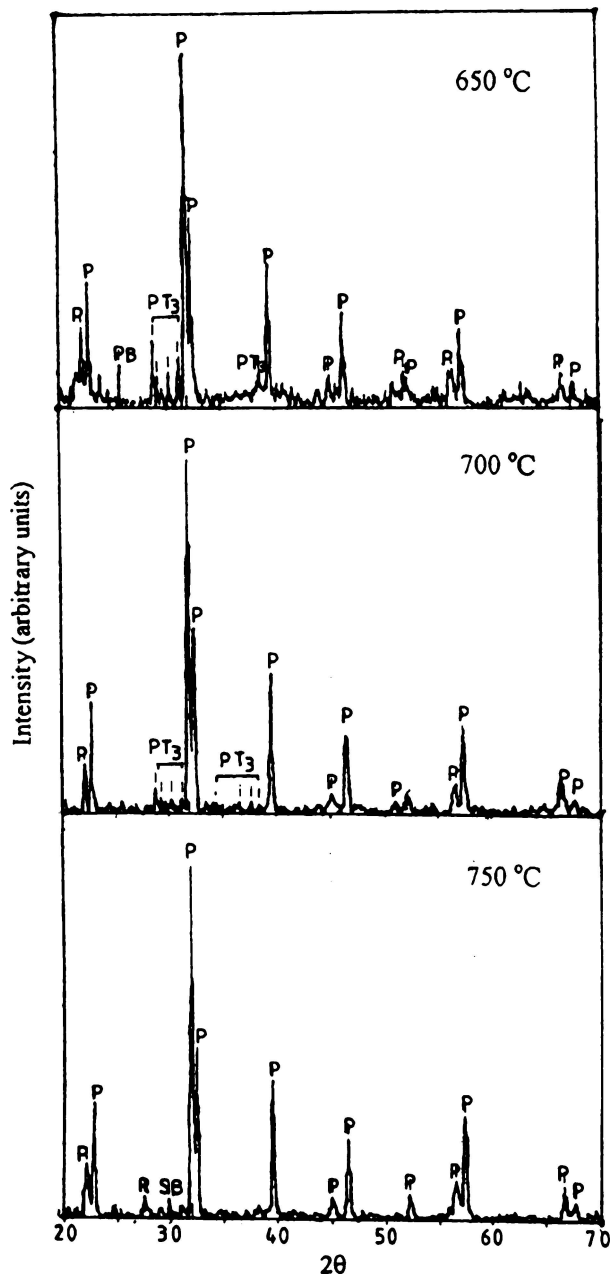


Figure 2 X-ray diffraction patterns of different glass ceramic samples of the glass $65[(\text{Pb}_{0.8}\text{Sr}_{0.2})\text{O}\cdot\text{TiO}_2] - 25[2\text{SiO}_2\cdot\text{B}_2\text{O}_3] - 5[\text{K}_2\text{O}] - 5[\text{BaO}]$ crystallized at different temperatures for 3 h.

The glass ceramics 6P5K700, 6P5K750 and 6P5K 800 prepared by crystallizing 6P5K glass were found to have perovskite titanate as the major phase. In addition to perovskite titanate, these glass ceramic samples were found to have a trace amount of PbTi_3O_7 and/or rutile phase. There is shift in XRD peak positions from that of undoped PbTiO_3 similar to glass ceramics discussed earlier. This is reflected in the value of their lattice parameters. The perovskite titanate phase developed in all the above three glass ceramic samples was found to have tetragonal crystal structure. The glass 6P5K was also heat treated at 750°C for 6 and 12 h. Perovskite titanate is found to be the only phase in 6 and 12 h heat treated samples, no

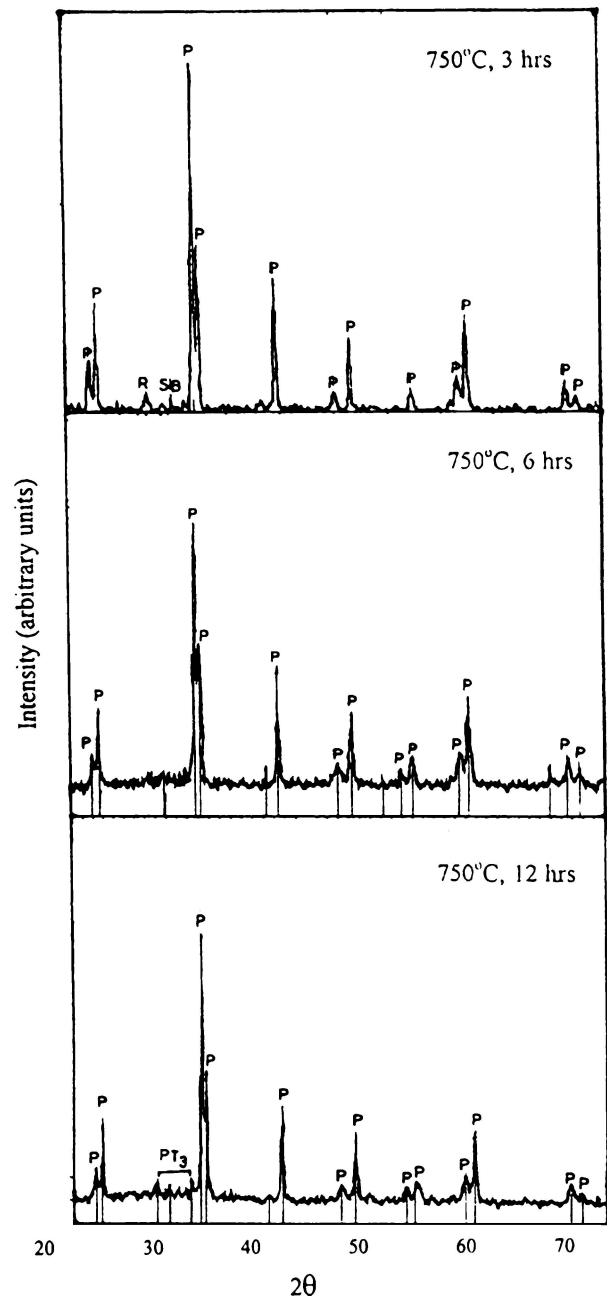


Figure 3 X-ray diffraction patterns of different glass ceramic samples of the glass $65[(\text{Pb}_{0.8}\text{Sr}_{0.2})\text{O}\cdot\text{TiO}_2] - 25[2\text{SiO}_2\cdot\text{B}_2\text{O}_3] - 5[\text{K}_2\text{O}] - 5[\text{BaO}]$ crystallized at 750°C for 3, 6 and 12 h.

minor phase was found to be present. The lattice parameters were not much affected by the extended duration of crystallization treatment. Powder XRD patterns of glass ceramic samples of glass 5P5K confirmed the formation of perovskite titanate as the major phase. Asymmetry of XRD peaks indicates very small tetragonality. PbTi_3O_7 , PbB_2O_4 and rutile (TiO_2) are the minor phases present in these glass ceramic samples.

All the glass ceramics obtained from strontium rich glasses 4P5K, 3P5K, 2P5K and 1P5K were found to have perovskite titanate as the major phase. The perovskite titanate phase developed in all these glass ceramic

TABLE IV Structure, lattice parameter(s) of different glass ceramic samples in the system $[(\text{Pb}_{1-x}\text{Sr}_x)\text{O}\cdot\text{TiO}_2]\text{--}[\text{2SiO}_2\cdot\text{B}_2\text{O}_3]\text{--}[\text{K}_2\text{O}]\text{--}[\text{BaO}]$

Glass ceramic	Crystal structure	Lattice parameter(s)		Axial ratio (<i>c/a</i>)
		<i>c</i> (Å)	<i>a</i> (Å)	
8P5K750	Tetragonal	4.021 ± 0.002	3.912 ± 0.002	1.027
7P5K750	Tetragonal	3.984 ± 0.001	3.912 ± 0.001	1.018
6P5K750	Tetragonal	3.959 ± 0.005	3.917 ± 0.005	1.011
5P5K750	Tetragonal	3.935 ± 0.002	3.915 ± 0.002	1.005
4P5K850	Cubic	–	3.911 ± 0.001	–
3P5K850	Cubic	–	3.880 ± 0.004	–
2P5K850	Cubic	–	3.886 ± 0.003	–
1P5K850	Cubic	–	3.90 ± 0.001	–

samples was found to have cubic crystal structure. The details of phase constitution are given in Table II. The lattice parameter of constituent perovskite titanate phase (Table IV) was found to closely match with the reported values of corresponding ceramics with same $\text{Pb}^{2+}/\text{Sr}^{2+}$ ratio. To compare the magnitude of shift of XRD peak positions from that of undoped PbTiO_3 with SrO concentration, XRD patterns of glass ceramic samples obtained by heat treating lead rich glasses ($x \leq 0.5$) at 750°C for 3 h and strontium rich glasses ($x > 0.5$) at 850°C for 3 h are presented in Fig. 4. Table IV lists the value of lattice parameter(s) and axial ratio of glass ceramic samples. The ‘*c*’ value of the crystalline phase gradually decreases with *x*. Not much variation in ‘*a*’ value is observed. This data is presented graphically in Fig. 5.

Perovskite titanate was found to be the major phase in all the glass ceramics. The glass ceramics differ only in the nature of the minor phase (PbTi_3O_7 , TiO_2 rutile, $\text{Sr}_2\text{B}_2\text{O}_5$, PbB_2O_4), which varies from sample to sample. A shift of XRD peak positions for perovskite titanate phase from that of undoped lead titanate was observed for all the glass ceramic samples. The magnitude of the shift was found to vary systematically with composition of initial glass, i.e., with concentration of SrO. The lattice parameter(s) and crystal structure of the crystalline phase developed in glass ceramic samples were found to be in good agreement with the reported values of solid solution $\text{PbTiO}_3\text{--SrTiO}_3$ ceramic system [26]. It is known that the shift in peak positions from that of undoped PbTiO_3 could be due to two factors: solid solution with SrTiO_3 and/or strain due to crystal clamping since both these phenomena produce similar deviations in XRD pattern. Therefore, the effect of solid solution can not be separated from that of strain by X-ray diffraction technique alone. An alternative method of determining the crystal composition was used.

3.2.1. Variation of intensity of XRD peaks of $(\text{Pb}_{1-x}\text{Sr}_x)\text{TiO}_3$ with $\text{Pb}^{2+}/\text{Sr}^{2+}$ ratio

A few glass ceramic samples were selected to study the variation of intensity of various XRD lines of their crystalline perovskite phase with $\text{Pb}^{2+}/\text{Sr}^{2+}$ ratio in the glass composition and compare the observed intensity of different *hkl* planes with the calculated intensity of solid solution $(\text{Pb}_{1-x}\text{Sr}_x)\text{TiO}_3$ phase. It was assumed that the crystalline phase in the glass ceramic sample approximately have the same $\text{Pb}^{2+}/\text{Sr}^{2+}$ ratio as in the initial batch composition. The intensity for various XRD lines

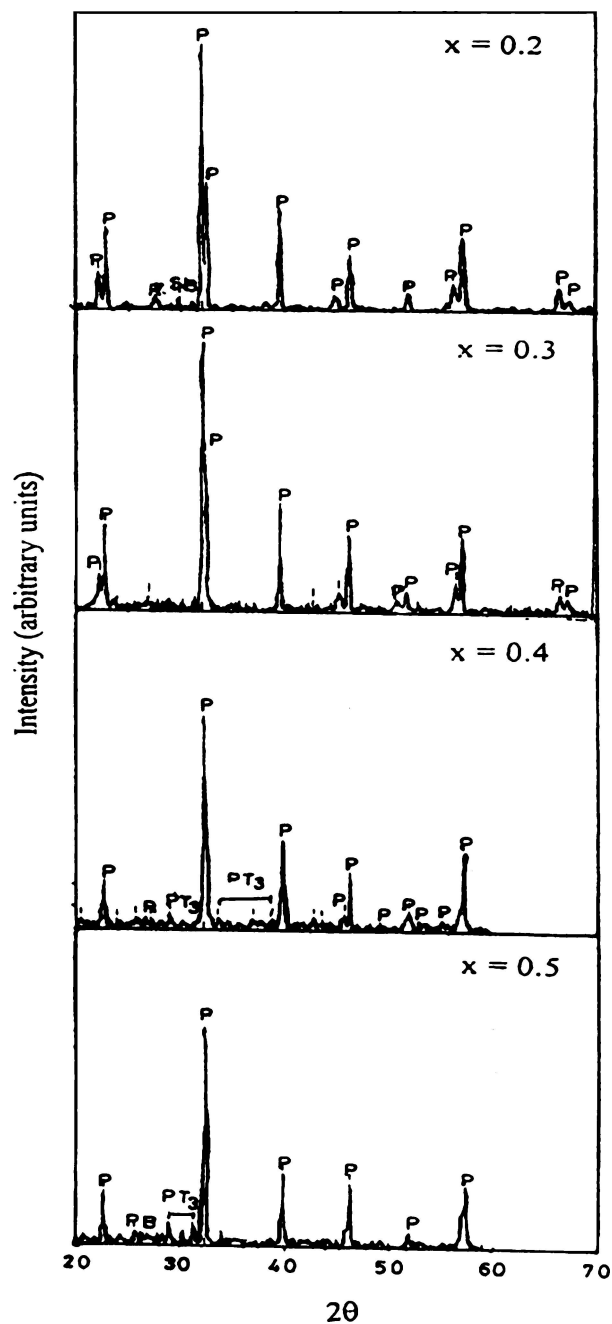


Figure 4 X-ray diffraction patterns of different glass ceramic samples in the system $65[(\text{Pb}_{1-x}\text{Sr}_x)\text{O}\cdot\text{TiO}_2]\text{--}25[\text{2SiO}_2\cdot\text{B}_2\text{O}_3]\text{--}5[\text{K}_2\text{O}]\text{--}5[\text{BaO}]$ crystallized at 750°C for 3 h.

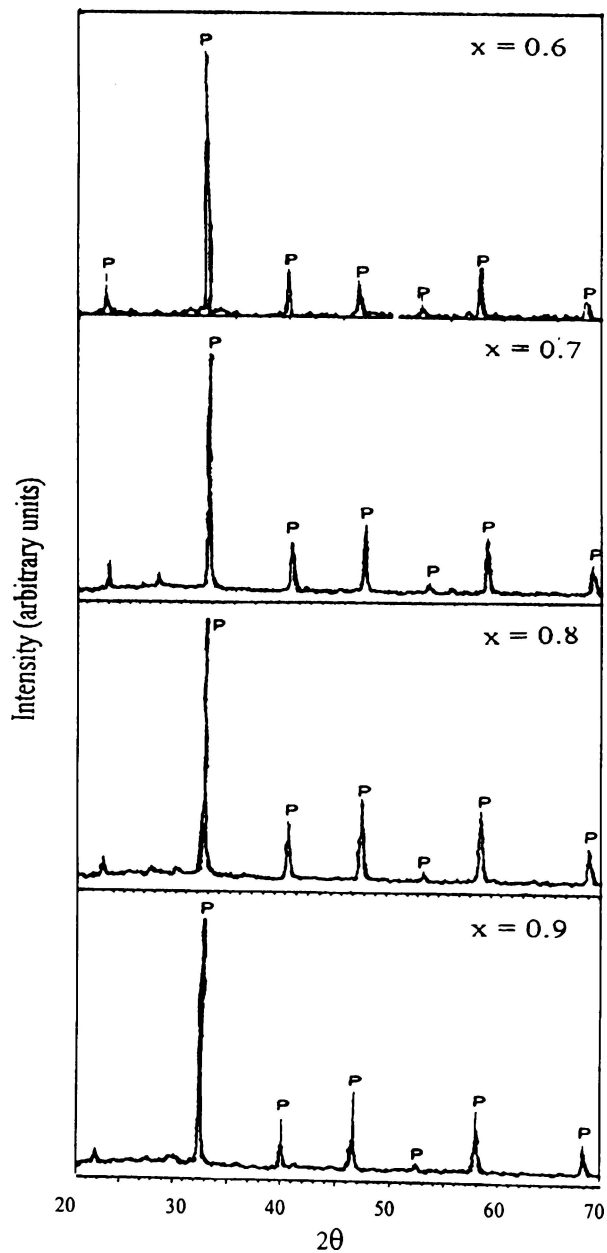


Figure 4 (continued.)

for different hkl planes for $(\text{Pb}_{1-x}\text{Sr}_x)\text{TiO}_3$ was calculated following the procedure described earlier [23]. Table Va gives the calculated intensity of various XRD lines for different hkl planes for the tetragonal $(\text{Pb}_{1-x}\text{Sr}_x)\text{TiO}_3$ solid solution perovskite composition ($x = 0.2, 0.3, 0.4$ and 0.5) along with the observed intensity of various XRD lines for different hkl planes for different glass ceramic samples with the same value of x . Similarly Table Vb shows the calculated intensity of various XRD lines for different hkl planes for cubic $(\text{Pb}_{1-x}\text{Sr}_x)\text{TiO}_3$ solid solution perovskite composition ($x = 0.6, 0.7, 0.8$ and 0.9) along with the observed intensity of various XRD lines for different hkl planes for different glass ceramic samples. The calculated and observed intensity of XRD peaks corresponding to (100) and (111) systematically decrease whereas that for (200) increases with $\text{Pb}^{2+}/\text{Sr}^{2+}$ ratio. For the remain-

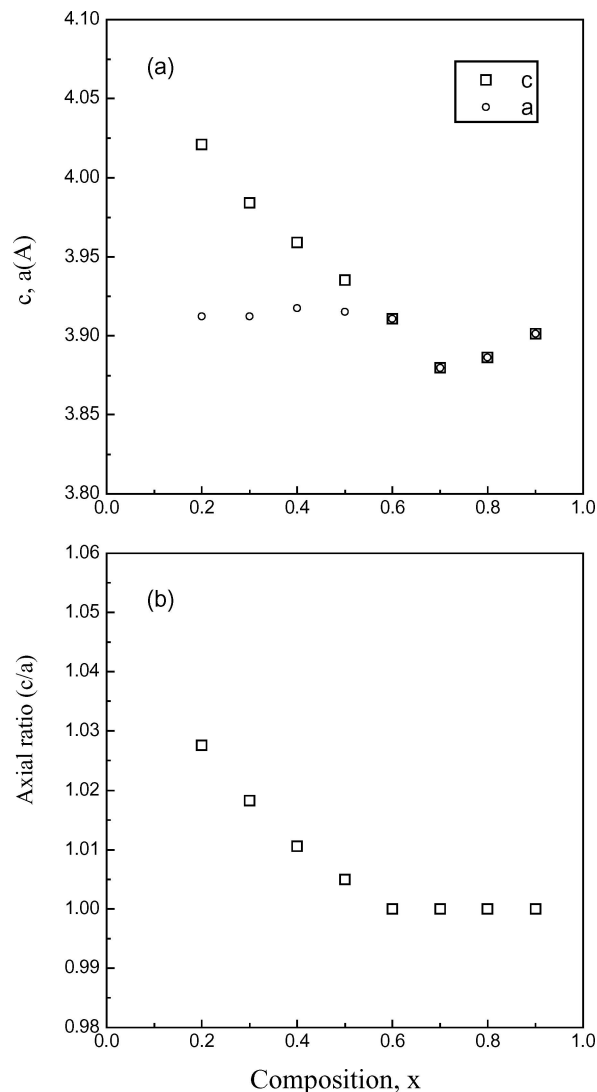


Figure 5 Variation of (a) lattice parameters and (b) axial ratio of crystalline phase developed by the crystallization of different glasses at 750°C for 3 h in the system $65[(\text{Pb}_{1-x}\text{Sr}_x)\text{O}\cdot\text{TiO}_2]-25[2\text{SiO}_2\cdot\text{B}_2\text{O}_3]-5[\text{K}_2\text{O}]-5[\text{BaO}]$.

ing reflections, both the intensities do not vary much with $\text{Pb}^{2+}/\text{Sr}^{2+}$ ratio. From Tables Va and b it is found that the calculated and observed intensity of different hkl planes of various glass ceramic samples follow the same trend with $\text{Pb}^{2+}/\text{Sr}^{2+}$ ratio as is observed in ceramic solid solution $(\text{Pb}_{1-x}\text{Sr}_x)\text{TiO}_3$. There is a little difference between the calculated and observed values and the difference is the maximum in case of the glass ceramic samples 5P5K800 and 4P5K850. This may be due to the fact that, the unit cell of the perovskite titanate phase has been considered as tetragonal and cubic for the glass ceramic samples 5P5K800 and 4P5K850 respectively and the indexing has been done accordingly. It is possible that both tetragonal and cubic phases coexist in these two samples. The calculated and the observed ratio of I_{111}/I_{200} are found to match and decrease with increasing $\text{Pb}^{2+}/\text{Sr}^{2+}$ ratio (Table VI) except for the glass ceramic 4P5K850. The reason may be the same for which the calculated and observed intensity of individual planes (111) and (200) differ.

TABLE VA Calculated and observed intensity of XRD peaks of tetragonal $(\text{Pb}_{1-x}\text{Sr}_x)\text{TiO}_3$ phase in different glass ceramic samples

hkl	8P5K750 ($x = 0.2$)		7P5K800 ($x = 0.3$)		6P5K800 ($x = 0.4$)		5P5K800 ($x = 0.5$)	
	I/I_0 (Cal)	I/I_0 (Obs)	I/I_0 (Cal)	I/I_0 (Obs)	I/I_0 (Cal)	I/I_0 (Obs)	I/I_0 (Cal)	I/I_0 (Obs)
001	14.6	14.6	11.6	11.7	–	–	–	–
100	27.4	32.1	22.2	25.4	19	29.4	15.6	19.2
101	100	100	100	100	100	100	100	100
110	52.5	48.8	48.9	57.2	–	–	–	–
111	49.4	39.2	44.7	53.2	38.8	41.3	43.2	27.9
002	17.9	5.9	16.5	9.9	16.7	12.3	–	–
200	32.4	21.9	30.9	32.5	32.1	32.7	33.3	22.5
201	–	–	8.7	14.1	8.4	7.3	7.0	6.3
210	10.2	6.7	–	–	7.8	12.3	–	–
112	22.0	10.5	20.0	19.6	–	–	–	–
211	42.1	28.6	38.5	44.8	38.7	32.4	38.7	26.9
202	20.2	9.0	18.7	8.7	19	10.1	–	–
220	9.6	4.8	–	–	–	–	–	–

 TABLE VB Calculated and observed intensity of XRD peaks of cubic $(\text{Pb}_{1-x}\text{Sr}_x)\text{TiO}_3$ phase in different glass ceramic samples

hkl	4P5K850 ($x = 0.6$)		3P5K850 ($x = 0.7$)		2P5K850 ($x = 0.8$)		1P5K850 ($x = 0.9$)	
	I/I_0 (Cal)	I/I_0 (Obs)	I/I_0 (Cal)	I/I_0 (Obs)	I/I_0 (Cal)	I/I_0 (Obs)	I/I_0 (Cal)	I/I_0 (Obs)
100	12.1	11.6	–	–	–	–	–	–
110	100	100	100	100	100	100	100	100
111	28.2	18.8	27.3	20.7	26.5	21.8	25.4	19.7
200	34.7	14.7	36.1	29.2	37.6	30.6	39.4	32.6
210	12.2	5.4	10.2	4.2	8.0	4.0	5.7	1.8
211	38.6	19.8	38.7	24.1	38.4	26.4	37.4	26.0
220	19.8	7.8	20.6	12.5	21.1	13.6	21.7	12.6

 TABLE VI Ratio of I_{111} and I_{200} (calculated and observed) for different glass ceramic samples

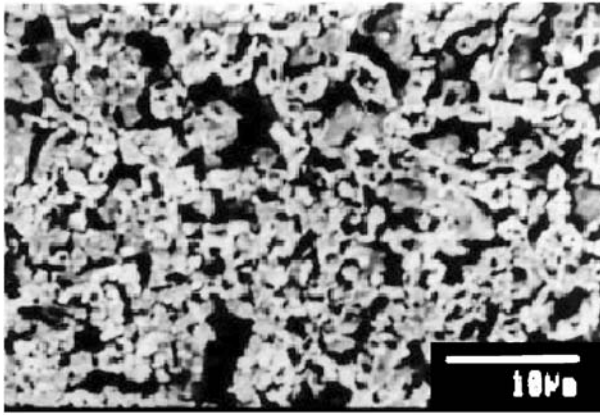
Glass ceramics	I_{111}/I_{200}	
	Calculated	Observed
8P5K750	1.524	1.789
7P5K800	1.446	1.636
6P5K800	1.208	1.262
5P5K800	1.297	1.240
4P5K850	0.812	1.278
3P5K850	0.756	0.708
2P5K850	0.704	0.712
1P5K850	0.644	0.604

The systematic and similar trend in variation of calculated and observed intensity with composition, x of $(\text{Pb}_{1-x}\text{Sr}_x)\text{TiO}_3$ solid solution ceramics and the perovskite titanate phase developed in glass ceramics indicates that lead-strontium titanate solid solution phase crystallized in the glass ceramic system.

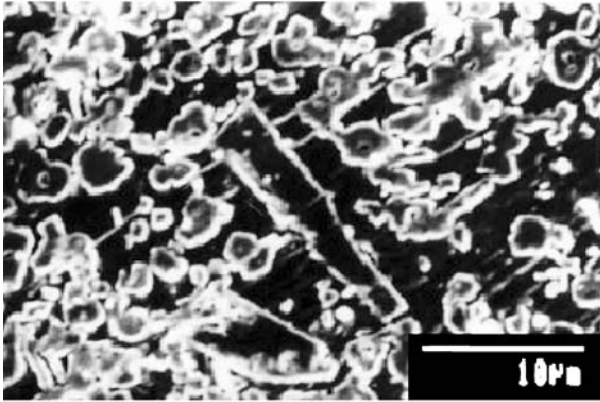
3.3. Microstructural studies

On the basis of observed microstructural characteristics, all the glass ceramic samples studied under present investigation can be categorized into three groups: (1) glass ceramic samples of 8P5K, (2) glass ceramic samples of 7P5K, 6P5K, 4P5K, 3P5K, 2P5K and (3) glass ceramic

samples of 1P5K. A few representative microstructures are presented in Figs 6–8. Fig. 6 shows the scanning electron micrographs of glass ceramic samples (8P5K700 and 8P5K750) obtained by heat treating the glass 8P5K at 700 and 750°C for 3 h. Microstructure of glass ceramic samples 8P5K700 shows fine crystallites of sub-micrometer size of perovskite titanate phase uniformly distributed in the glassy matrix. When the crystallization temperature is increased to 750°C, growth of crystallites occurs as in the case of 8P5K750, where the size of crystallites is found to be in the range 2–4 μm . In addition to spherical crystallites, a few elongated crystallites are also seen. The microstructure of glass ceramic sample 7P5K750 consists of interconnected crystallites (Fig. 7a). Fig. 7b shows scanning electron micrograph of glass ceramic sample 6P5K800. The microstructure is similar to that of 7P5K750 with the difference that a few crystallites are also observed with different morphology. These crystallites may be of minor phases ($\text{PbTi}_3\text{O}_7/\text{TiO}_2$ -rutile). Interconnecting crystallites are also observed for glass ceramic sample 5P5K800 and 4P5K750 (Fig. 7c and d). The microstructural characteristics of the glass ceramic 3P5K800 (Fig. 7e) and 2P5K800 (Fig. 7f) were found to be similar to that of 4P5K750. Generally, interconnected crystallites type of microstructure is observed in glass ceramics where glass-in-glass phase separation takes place prior to crystallization [18]. The crystallization behaviour of these glasses based on the coordination



(a)



(b)

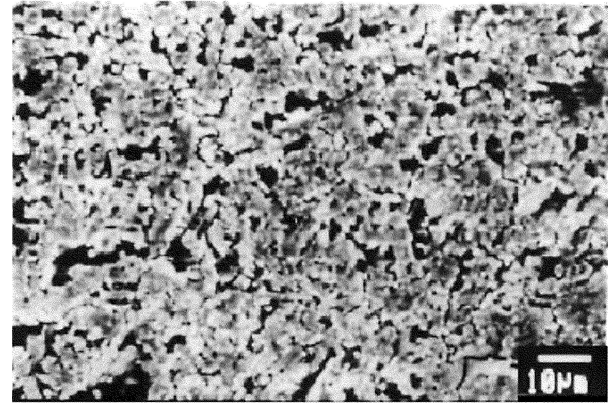
Figure 6 Scanning electron micrographs of chemically etched surfaces of glass ceramic samples (a) 8P5K700 and (b) 8P5K750.

structure of various constituent ions can be explained as follows:

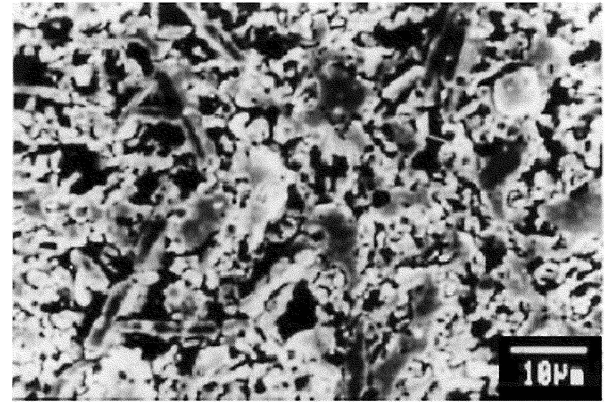
The borosilicate glass structure generally consists of SiO_4 , BO_3 and BO_4 network forming units linked through the oxygen. B–O–B, Si–O–Si and B–O–Si bond linkages are present in the glassy network. The presence of such bonds is identified by Infrared spectroscopy (IR) and solid state Nuclear Magnetic Resonance (NMR) techniques. In borosilicate glass, with the addition of modifier alkali (K^+) or alkaline earth ions (Sr^{2+} , Ba^{2+}) these linkages are broken giving rise to non-bridging oxygen (NBO) ions. In high PbO containing glasses the coordination number of Pb is three suggesting that PbO acts as a network former consisting of PbO_3 trigonal pyramids. These pyramids are connected to other structural units in the glassy network. When the content of PbO is small they act as network modifier with six coordinated Pb ions [27]. TiO_2 is generally present as TiO_6 octahedra, may also participate in the glass structure leading to formation of Si–O–Ti, B–O–Ti and Ti–O–Ti bonds in the glass structure. The randomness of glass network is attributed to flexibility of Si–O–Si bond angles etc. The interconnected octahedrally coordinated Ti^{4+} ions (Ti–O–Ti bond angle) lack such flexibility of bond angles. When the concentration of these cations are high and their coordination polyhedra is not associated

with a true network former as their nearest neighbours, they become structurally ordered with respect to each other. These structurally ordered regions produce microheterogeneities in the glass structure which may lead to glass-in-glass phase separation during the heat treatment of the glass. The phase separation influences nucleation and crystallization of glass and hence the microstructure of resulting glass ceramics [28].

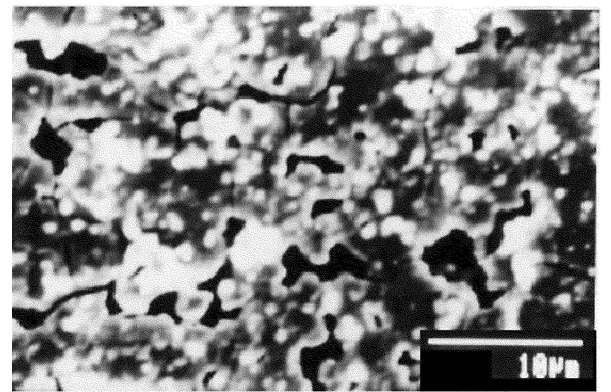
Fig. 8 shows scanning electron micrograph of 1P5K800. It shows fine crystallites of $1 \mu\text{m}$ uniformly



(a)

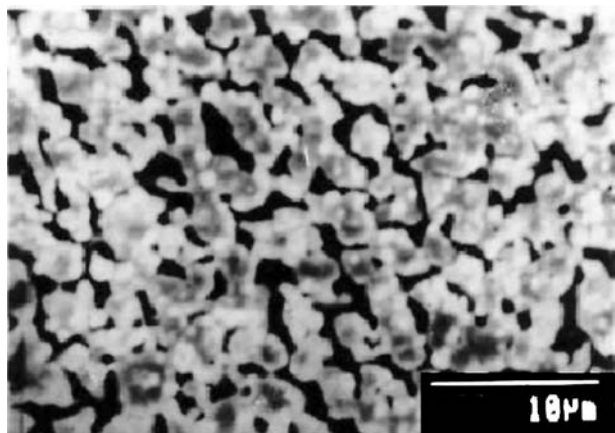


(b)

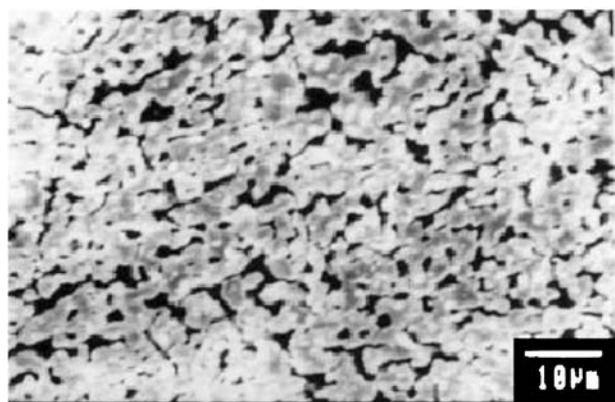


(c)

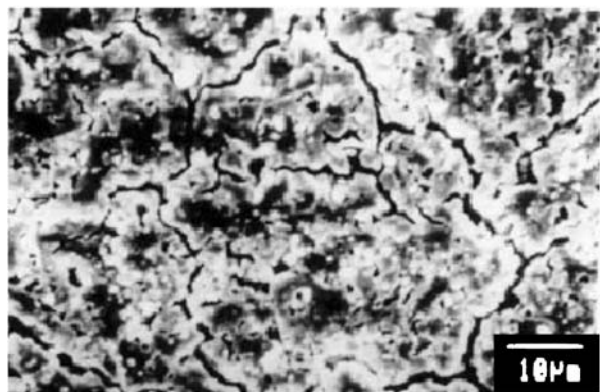
Figure 7 Scanning electron micrographs of chemically etched surfaces of glass ceramic samples. (a) 7P5K750, (b) 6P5K800, (c) 5P5K800, (d) 4P5K750, (e) 3P5K800 and (f) 2P5K800.



(d)



(e)



(f)

Figure 7 (Continued.)

distributed throughout the matrix. No interconnectivity of the crystallites was observed. This means that degree of phase separation is small and rate of nucleation and crystal growth may be higher. This gives rise to fine grained microstructure in this sample during the crystallization treatment.

From the microstructural observation of these glass ceramic samples, the inference may be drawn that in lead rich and strontium rich glasses (8P5K and 1P5K) the degree of phase separation is smaller and rate of crystallization is higher during heat treatment. Hence high cooling rate is required during the quenching of the melt to get

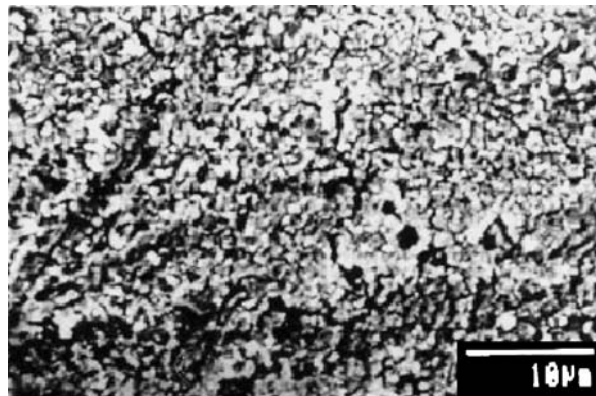


Figure 8 Scanning electron micrographs of chemically etched surfaces of glass ceramic sample 1P5K800.

bulk transparent glasses. This might be one of the reasons for the difficulty in glass forming of these compositions. In the intermediate compositions, i.e., when the Pb^{2+}/Sr^{2+} ratio is 1 or nearly one, glass-in-glass phase separation takes place during the early stage of crystallization treatment. This also makes the glass formation easy with a relatively low cooling rate.

4. Conclusions

The phase development and microstructural characteristics of various glass ceramic samples in the $[(Pb_{1-x}Sr_x)O \cdot TiO_2] - [2SiO_2 \cdot B_2O_3] - [K_2O] - [BaO]$ system have been investigated. Bulk transparent glasses in this system could be prepared. Perovskite titanate was found to be major phase in all the glass ceramic samples. A shift in the XRD peak positions from that of undoped $PbTiO_3$ was observed. Crystalline phase of all the glass ceramic samples of glasses with $x \leq 0.5$ was found to have tetragonal structure whereas for $x > 0.5$ cubic structure was observed. The lattice parameter(s) and axial ratio were less influenced by crystallization temperature and time for a fixed SrO concentration in the glass. However, a systematic variation in 'c', 'a' and c/a was observed with increasing SrO concentration. The observed intensity of different hkl planes of various glass ceramic samples and calculated intensity of $(Pb_{1-x}Sr_x)TiO_3$ ceramics were found to vary in a systematic way with change in Pb^{2+}/Sr^{2+} ratio and similar trend was observed for both. Thus the composition of the crystallites was confirmed to be $(Pb_{1-x}Sr_x)TiO_3$ solid solution. Microstructure of most of the glass ceramics developed consists of interconnected crystallites which are desired for better performance as capacitor material. Fine crystallites, uniformly distributed through the glassy matrix are the characteristic feature of microstructure of some of the glass ceramic samples.

Acknowledgments

The authors thank Dr. Lakshman Tiwari of the Research and Development Centre for Iron and Steel, Ranchi, India for extending DTA facility and the Incharge, National

Electron Microscope Facility, Department of Metallurgical Engineering, Banaras Hindu University, Varanasi for providing scanning electron microscope facility.

References

1. P. W. MCMILLAN, in "Glass-Ceramics" (Academic Press, London, 1979) p. 4.
2. C. G. BERGERON and C. K. RUSSELL, *J. Am. Ceram. Soc.* **48** (1965) 115.
3. D. G. GROSSMAN and J. O. ISARD, *ibid.* **52** (1969) 230.
4. *Idem.*, *J. Mater. Sci.* **4** (1969) 1059.
5. S. M. LYNCH and J. E. SHELBY, *J. Am. Ceram. Soc.* **67** (1984) 424.
6. T. KOKUBO and M. TASHIRO, *J. Non-Cryst. Solids* **13** (1973/74) 328.
7. WU MIANXUE and ZHU PEINAN, *ibid.* **84** (1986) 344.
8. JIIN-JYH SHYU and YEONG-SONG YANG, *J. Am. Ceram. Soc.* **78** (1995) 1463.
9. K. SAEGUSA, *ibid.* **79** (1996) 3282.
10. W. N. LAWLESS, *Ferroelectrics* **3** (1972) 287.
11. *Idem.*, *ibid.* **7** (1974) 379.
12. S. L. SWARTZ, M. T. LANAGAN, W. A. SCHULZE and L. E. CROSS, *ibid.* **50** (1983) 313.
13. S. L. SWARTZ, A. S. BHALLA, L. E. CROSS, C. F. CLARK and W. N. LAWLESS, *J. Appl. Phys.* **60** (1986) 2069.
14. S. L. SWARTZ, E. BREVAL and A. S. BHALLA, *Am. Ceram. Soc. Bull.* **67** (1988) 763.
15. S. L. SWARTZ, E. BREVAL, C. A. RANDALL and B. H. FOX, *J. Mater. Sci.* **23** (1988) 3997.
16. S. L. SWARTZ, A. S. BHALLA, L. E. CROSS and W. N. LAWLESS, *ibid.* **23** (1988) 4004.
17. O. P. THAKUR, in "Crystallization, Microstructure and Dielectric Behaviour of Strontium Titanate Borosilicate Glass Ceramics with Some Additives," Ph.D. Thesis, Banaras Hindu University, Varanasi, India, 1998.
18. O. P. THAKUR, D. KUMAR, O. PARKASH and L. PANDEY, *Mater. Letts.* **23** (1995) 253.
19. A. K. SAHU, D. KUMAR, O. PARKASH, O. P. THAKUR and C. PRAKASH, *Ceram. Int.* **30** (2004) 477.
20. R. K. MANDAL, C. DURGA PRASAD, O. PARKASH and D. KUMAR, *Bull. Mater. Sci.* **9** (1987) 255.
21. R. BHATTACHARYA, in "Preparation & Characterization of Strontium-Lead Titanate ($\text{Sr}_{1-x}\text{Pb}_x\text{TiO}_3$) Borosilicate Glass-ceramic System", M. Tech. Dissertation, Banaras Hindu University, Varanasi, India, 1996.
22. M. BEHERA, in "Preparation and Characterization of Barium-Strontium —Titanate Borosilicate Glass Ceramic System," M.Tech. Dissertation, Banaras Hindu University, Varanasi, India, 1998.
23. ASHOK K. SAHU, DEVENDRA KUMAR and OM PARKASH THAKUR, *Brit. Ceram. Trans.* **102** (2003) 139.
24. A. K. SAHU, D. KUMAR, O. PARKASH, O. P. THAKUR and C. PRAKASH, *ibid.* **102** (2003) 148.
25. B. D. CULITY, in "Elements of X-Ray Diffraction" (Addison-Wesley Publishing Company, inc., California, 1978) p. 520.
26. S. SUBRAHMANYAM and E. GOO, *Acta. Mater.* **46** (1998) 817.
27. T. TAKAISHI, J. JIN, T. UCHINO and T. YOKO, *J. Am. Ceram. Soc.* **83** (2000) 2543.
28. O. PARKASH, D. KUMAR and L. PANDEY, *Bull. Mater. Sci.* **8** (1986) 557.

Received 27 February 2004
and accepted 17 May 2005